

and an ILU(0) factorization of the distance-1 Jacobian matrix is used as a preconditioner for the linear system. As shown in Figs. 3b and 3c, a fast convergence is achieved on both grids for the two turbulence models, thus demonstrating the high efficiency of the Newton–Krylov approach.

Conclusions

An efficient pseudotransient Newton–Krylov algorithm has been described and applied to the solution of steady-state compressible turbulent flows around two-dimensional wing configurations. Computations of several turbulent flows have shown that 1) the strong coupling of the turbulence model with the averaged Navier–Stokes equations permits a Newton-type convergence for all the equations; 2) the use of a mesh sequencing strategy greatly reduces the number of nonlinear iterations and the computational time; 3) the choice of an ILU(0) factorization of the distance-1 Jacobian matrix as a preconditioner generally results in a good compromise between computational time and memory requirements; 4) if the memory requirements are not essential, the choice of a higher value of the level of fill-in can greatly increase the performance of the Krylov solver; and 5) the computational time required for one steady-state calculation is equal to the cost of a few thousand evaluations of the nonlinear residual. This makes the present solution strategy highly competitive with state-of-the-art multigrid techniques.

Acknowledgments

This research was supported by the Belgian Industry and Agriculture Research Training Fund while the author was Research Assistant at the Aerodynamics Group of the University of Liège, Belgium.

References

- McHugh, P. R., and Knoll, D. A., "Comparison of Standard and Matrix-Free Implementations of Several Newton–Krylov Solvers," *AIAA Journal*, Vol. 32, No. 12, 1994, pp. 2394–2400.
- Nielsen, E. J., Anderson, W. K., Walters, R. W., and Keyes, D. E., "Application of Newton–Krylov Methodology to a Three-Dimensional Unstructured Euler Code," AIAA Paper 95-1733, 1995.
- Pueyo, A., and Zingg, D. W., "Efficient Newton–Krylov Solver for Aerodynamic Computations," *AIAA Journal*, Vol. 36, No. 11, 1998, pp. 1991–1997.
- Barth, T. J., and Linton, S. W., "An Unstructured Mesh Newton Solver for Compressible Fluid Flow and its Parallel Implementation," AIAA Paper 95-0221, 1995.
- Geuzaine, P., Lepot, I., Meers, F., and Essers, J.-A., "Multilevel Newton–Krylov Algorithms for Computing Compressible Flows on Unstructured Meshes," AIAA Paper 99-3341, 1999.
- Geuzaine, P., "An Implicit Upwind Finite Volume Method for Compressible Turbulent Flows on Unstructured Meshes," Ph.D. Dissertation, University of Liège, Liège, Belgium, 1999.
- Spalart, P. R., and Allmaras, S. R., "One-Equation Turbulence Model for Aerodynamic Flows," AIAA Paper 92-0439, 1992.
- Wilcox, D. C., "Reassessment of the Scale-Determining Equation for Advanced Turbulence Models," *AIAA Journal*, Vol. 26, No. 11, 1988, pp. 1299–1310.
- Delanaye, M., Geuzaine, P., and Essers, J.-A., "Development and Application of Quadratic Reconstruction Schemes for Compressible Flows on Unstructured Adaptive Grids," AIAA Paper 97-2120, 1997.
- Geuzaine, P., Delanaye, M., and Essers, J.-A., "Computations of High Reynolds Number Flows with an Implicit Quadratic Reconstruction Scheme on Unstructured Grids," AIAA Paper 97-1947, 1997.
- Saad, Y., and Schultz, M. H., "GMRES: a Generalized Minimal Residual Algorithm for Solving Nonsymmetric Linear Problems," *SIAM Journal on Scientific and Statistical Computing*, Vol. 7, No. 3, 1986, pp. 856–869.
- Thibert, J. J., Grandjacques, M., and Ohman, L. H., "NACA 0012," *Experimental Data Base for Computer Program Assessment*, AR-138, AGARD, 1979, Chap. 1.
- Cook, P. H., McDonald, M. A., and Firmin, M. C. P., "Aerofoil RAE 2822—Pressure Distribution, and Boundary Layer, and Wake Measurements," *Experimental Data Base for Computer Program Assessment*, AR-138, AGARD, 1979, Chap. 6.
- van den Berg, B., "Boundary Layer Measurements on a Two-Dimensional Wing with Flap," National Aerospace Lab., TR NLR TR-79009 U, The Netherlands, 1979.

J. Kallinderis
Associate Editor

Characteristics of a Plunging Airfoil at Zero Freestream Velocity

Joseph C. S. Lai*

University of New South Wales,
Australian Defence Force Academy, Canberra,
Australian Capital Territory 2600, Australia

and

Max F. Platzer†

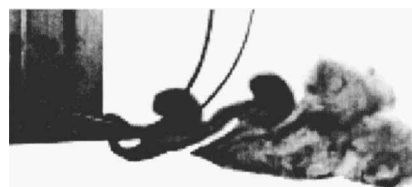
Naval Postgraduate School,
Monterey, California 93943-5106

Nomenclature

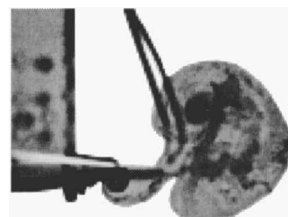
a	=	amplitude of oscillation, mm
c	=	chord of airfoil, mm
d	=	diameter of cylinder, mm
f	=	frequency of oscillation, Hz
h	=	nondimensional amplitude of oscillation, a/c
k	=	reduced frequency parameter, $2\pi fc/U_0$
kh	=	nondimensional plunge velocity, $2\pi fa/U_0$
U	=	mean streamwise velocity
U_{\max}	=	maximum streamwise velocity
U_0	=	freestream velocity
V_p	=	peak plunge velocity, $2\pi fa$, m/s
x	=	streamwise direction measured from the trailing edge
y	=	lateral direction measured from the centerline of the airfoil
y_{\max}	=	location where $U = U_{\max}$

I. Introduction

Flows around oscillating airfoils are relevant for the analysis of aircraft wing flutter, helicopter and turbomachine blade flutter, and for the prediction of aeroacoustic noise generation. The analysis of incompressible flow past oscillating airfoils was



a) $f = 10$ Hz, $k = 31.4$ ($kh = 0.785$), and $U_0 = 0.2$ m/s



b) $f = 2.5$ Hz, $h = 0.025$, and $U_0 = 0$ m/s

Fig. 1 Vortex patterns for a 100-mm NACA 0012 airfoil oscillated in plunge for $h = 0.025$ and various frequencies of oscillation.

Received 1 October 1999; revision received 6 November 2000; accepted for publication 7 November 2000. This material is declared a work of the U.S. Government and is not subject to copyright protection in the United States.

*Associate Professor, School of Aerospace and Mechanical Engineering, University College. Senior Member AIAA.

†Professor, Department of Aeronautics and Astronautics; platzer@aa.nps.navy.mil. Fellow AIAA.

pioneered by Birnbaum¹ in the 1920s, followed by Theodorsen² and Garrick,³ to study aeroelastic flutter problems. These flows have also attracted significant attention in biohydrodynamics because of the need to understand the propulsion mechanisms⁴ of aquatic animals, birds, and insects. Whereas a pitching airfoil oscillates about a pivot, resulting in different angles of incidence at different phases of the oscillation, a plunging or flapping airfoil is one in which the airfoil is displaced periodically in the vertical direction with its orientation fixed relative to a fixed frame of reference. Although the wake patterns behind airfoils undergoing small-amplitude pitching and plunging oscillations have been studied quite extensively,^{5,6} the velocity field of an airfoil undergoing pure plunging motion has not been explored in any detail until recently.⁷

It was first recognized by Knoller,⁸ and later independently by Betz,⁹ that a flapping airfoil generates thrust. Bennett et al.¹⁰ per-

formed some ornithopter aerodynamic experiments and confirmed that thrust was produced by flapping a two-dimensional NACA 0014 airfoil. Preliminary flow visualization and laser Doppler velocimetry (LDV) studies by Jones et al.¹¹ have enabled the excitation to be classified as drag producing, neutral, or thrust producing in terms of the excitation frequency and amplitude.

The flow characteristics of a plunging airfoil at zero freestream velocity are of fundamental and applied interest because they aid in understanding the thrust generation accomplished by many insects and small birds for sustained hovering in still air,¹² the aerodynamics of ornithopter¹⁰ and micro air vehicles.¹³ Various hovering modes¹² (i.e. thrust generation in a still fluid environment) including the water treading mode, normal hovering mode, oblique or dragonfly mode, and the oriental fan mode of pure pitching have been investigated using flow visualization, but pure plunging has not been considered

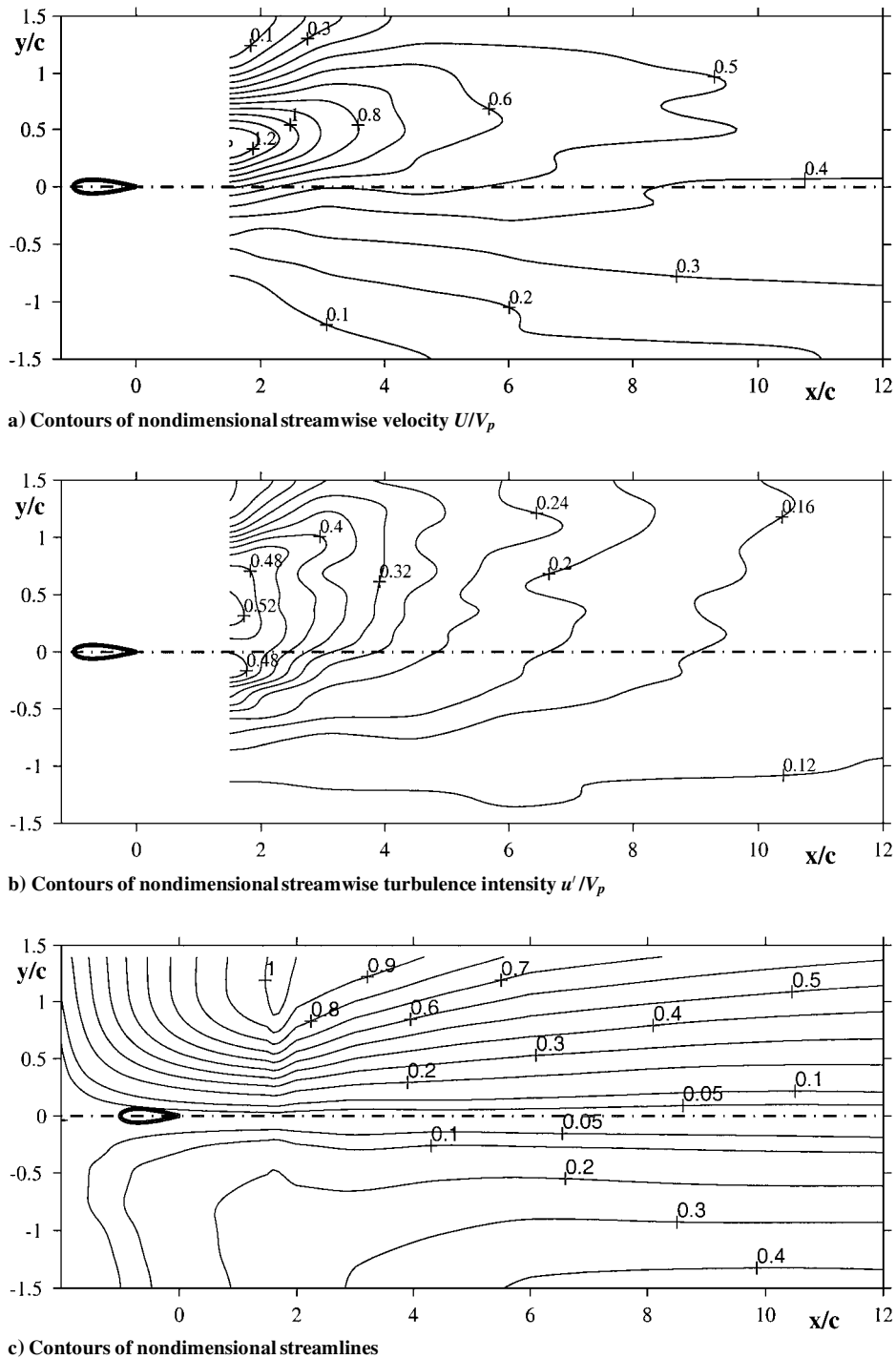


Fig. 2 Mean velocity field for a flapping 10-mm chord NACA 0012 airfoil: $f = 10$ Hz, $h = 0.247$ and $U_0 = 0$.

in this context. The objective of this study was, therefore, to examine the mean streamwise velocity field of the wake of a NACA 0012 airfoil oscillated in plunge at zero freestream velocity and at zero angle of incidence at the neutral position.

II. Consideration of Relevant Parameters

For a given airfoil oscillating in plunge at nonzero freestream velocity, the relevant parameters that determine the wake structures include the frequency of oscillation f , the amplitude of oscillation a , the chord c of the airfoil, and the freestream velocity U_0 . Consequently, the relevant nondimensional parameters are the nondimensional reduced frequency, $k = 2\pi fc/U_0$; the nondimensional amplitude of oscillation, $h = a/c$; and the nondimensional plunge velocity, $kh = 2\pi fa/U_0$. By the measurement of the mean streamwise velocity field of a NACA 0012 airfoil oscillated in plunge for a range of nonzero freestream velocities, frequencies, and amplitudes of oscillation, Lai and Platzer⁷ have shown that when kh exceeds approximately 0.25 a jet instead of a wake is produced downstream of the plunging airfoil. Furthermore, the nondimensional maximum mean streamwise velocity data have been shown to vary linearly with kh .

When the freestream velocity U_0 is zero, both k and kh assume infinite values and are undefined. Under this condition, the only velocity scale is the peak plunge velocity, $V_p = 2\pi fa$, and the relevant length scales are the chord c and the amplitude of oscillation a . A nondimensional frequency parameter can be defined as $2\pi fc/V_p$ or $2\pi fa/V_p$, which reduces to c/a or 1, respectively, thus implying that the wake of a plunging airfoil at zero freestream velocity is independent of the frequency of oscillation. It can, therefore, be argued that for zero freestream velocity, the mean velocity profiles should be independent of the frequency of oscillation if the velocities are nondimensionalized by V_p and the lateral distance is nondimensionalized by a . Note that Freymuth¹² has chosen to include the influence of frequency in a Reynolds number based on the plunge velocity V_p , chord c , and the kinematic viscosity ν of the fluid.

III. Experimental Setup and Instrumentation

All of the experiments were conducted in a closed-circuit continuous-flow water-tunnel facility with a contraction ratio of 6:1. The test section is 380 mm wide, 1500 mm long, and 510 mm high. Whereas the top of the test section is open to atmosphere, the remaining three sides are made of glass to provide optical access for flow visualization and LDV measurements. The flow velocity can be adjusted in a range from 0 to about 0.5 m/s.

Experiments were conducted using two NACA 0012 airfoils, each with a span of 355 mm. The larger airfoil with a chord c of 100 mm was primarily used for measurements in the near field, close to the trailing edge, whereas the smaller airfoil with a chord c of 10 mm was used for measurements in the far field. A shaker was mounted on top of the test section to oscillate the airfoil sinusoidally in plunge. The signal from a frequency generator was varied from 2.5 to 10 Hz. The amplitude of oscillation, measured with a linear variable differential transformer, was varied primarily from 2.5 to 8 mm.

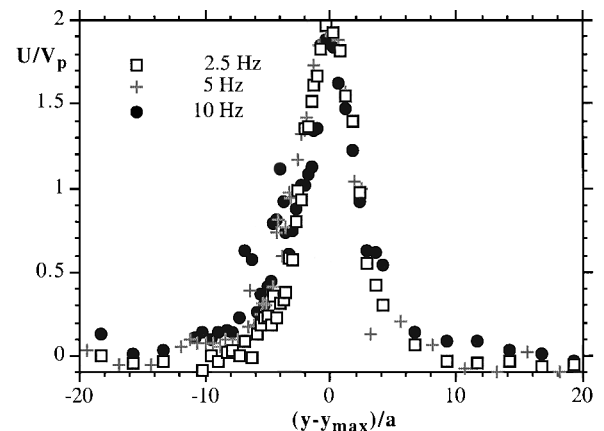
A TSI, Inc., single-component LDV was used to measure the mean streamwise velocity and streamwise turbulence intensity distributions up to 12 chord lengths downstream of the trailing edge of the airfoil. The fiber optic probe head could be traversed with an accuracy of 0.1 mm in the streamwise x , transverse y , and spanwise z directions. The light source was an Omnichrome Model 543-300A argon ion laser with a rated output of 300 mW at 8.8 Å. The beam separation was 50 mm and the focal length was 350 mm, giving a fringe spacing of $3.427 \mu\text{m}$ for the blue beam. The Doppler signal was processed with a TSI IFA 550 intelligent flow processor. The data acquisition was automated using a personal computer and TSI flow information display (FIND) software. At least 1000 data samples were used for each measurement point. Although the maximum differences between corrected and uncorrected data were less than 2%, velocity correction based on time between data was

applied. Uncertainty estimates indicate that the uncertainty in the mean velocity measurements is within $\pm 5 \text{ mm/s}$.

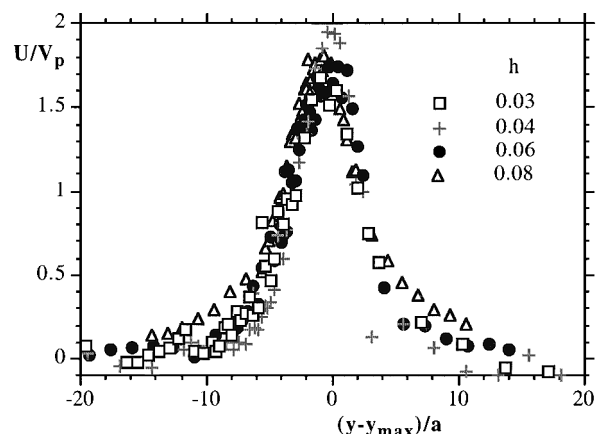
IV. Results

Dye flow visualization was used to illustrate the vortex street downstream of a 100-mm chord NACA 0012 airfoil oscillated in plunge. The vortex patterns at $U_0 = 0.2 \text{ m/s}$ for $h = 0.025$ and $f = 0, 2.5, 5$, and 10 Hz have been documented by Lai and Platzer.⁷ These results show that, as kh is increased to greater than 0.2, the vortex pattern changes from a drag-producing wake to a thrust-producing wake. At large kh such as 0.785, Fig. 1a shows that the axis of the thrust-producing vortex street is no longer aligned with the chord axis at the airfoil's neutral position; instead, it is inclined at an angle pointing upward relative to the chord axis. When $U_0 = 0$ and the airfoil is oscillated in plunge at $f = 2.5 \text{ Hz}$ and $h = 0.025$, Fig. 1b shows that the resulting vortex pattern is jetlike, but that the axis of the vortex street is inclined, similar to that for large kh and nonzero U_0 shown in Fig. 1a.

Figures 2a and 2b display contours of nondimensional streamwise velocity U/V_p and streamwise turbulence intensity u'/V_p , respectively, when a 10-mm NACA 0012 airfoil is oscillated in plunge at zero angle of incidence with $f = 10 \text{ Hz}$, $h = 0.247$, and $U_0 = 0$. Figure 2a shows that, although the freestream velocity is zero, a jet is produced by the flapping airfoil with a streamwise velocity greater than the peak plunge velocity V_p for up to almost three chord lengths downstream of the trailing edge of the airfoil. The jet appears to be biased toward the half-plane above the airfoil, consistent with the vortex pattern identified by flow visualization in Fig. 1. This phenomenon has been observed before by Jones et al.¹¹ As soon as kh exceeds approximately 0.8, the vortices shed from the trailing edge are coming too close together¹¹ and start to interact



a) $h = 0.04$

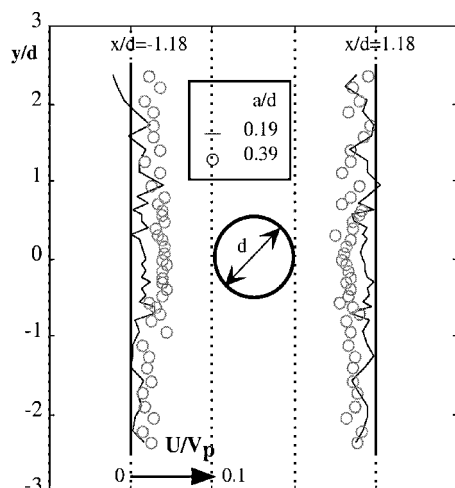


b) $f = 5 \text{ Hz}$

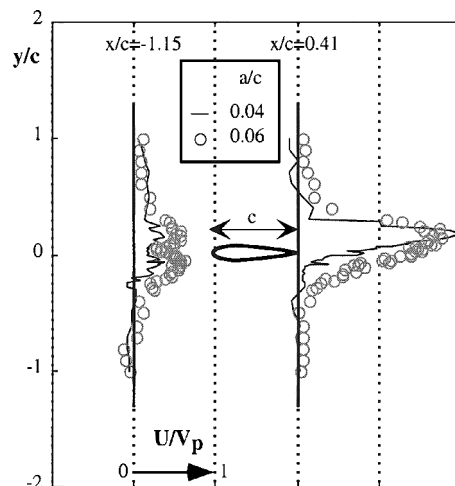
Fig. 3 Nondimensional streamwise velocity profiles at $x/c = 0.41$ and $U_0 = 0$.

with each other nonlinearly. The resulting jet is deflected upward or downward depending on the direction of the starting motion of the airfoil. The experimental observations are predicted well by a potential flow solver¹¹ and a Navier–Stokes code.¹⁴ Further studies are required to determine whether leading-edge separation plays a role in producing asymmetric vortex shedding. The streamwise turbulence intensity contours in Fig. 2b are typical of a jet. Although the jet is not symmetrical with respect to the mean chord axis, and the velocity measurements have been made with a single component LDV, approximate streamline contours may be estimated by integrating the mean streamwise velocity field in Fig. 2a by assuming that there is no flow across the mean chord axis. As shown in Fig. 2c, the streamline contours thus obtained do indicate that the jet is biased toward the half-plane above the airfoil's neutral position.

Nondimensional streamwise velocity profiles U/V_p measured at $x/c = 0.41$ downstream of a 100-mm NACA 0012 airfoil for $h = 0.04$ and $f = 2.5, 5$, and 10 Hz and for $f = 5$ Hz and $h = 0.03, 0.4, 0.06$, and 0.08 are displayed in Figs. 3a and 3b, respectively. Within the limits of experimental accuracy, Fig. 3a shows that for a given h , the velocity profiles for different frequencies fall onto each other, thus indicating independence of the frequency of oscillation for $U_0 = 0$. These results confirm the analysis of the relevant parameters for $U_0 = 0$. Furthermore, Fig. 3b indicates that for a given frequency, the velocity profiles are also independent of h when the lateral distance is nondimensionalized using the amplitude of oscillation a .



a) Cylinder of diameter 12.65 mm



b) 100-mm chord NACA 0012 airfoil

Fig. 4 Nondimensional mean streamwise velocity profiles for $f = 5$ Hz and two different amplitudes of oscillation at $U_0 = 0$.

Bennett et al.¹⁰ attributed the thrust generation in still air of a plunging airfoil to the asymmetry between the round leading and sharp trailing edges of the airfoil. Thus, experiments were conducted to measure the mean streamwise velocity profiles upstream and downstream of a 12.65-mm-diam circular cylinder and a 100-mm NACA 0012 airfoil oscillated in plunge at $U_0 = 0$. For the circular cylinder oscillated at $f = 5$ Hz with two different amplitudes, $a = 0.19d$ and $0.39d$, Fig. 4a clearly shows that no jet is produced under the oscillation. It may be inferred from Fig. 4a that the mean streamwise velocity field for the plunging cylinder resembles that of a quadrupole. On the other hand, Fig. 4b shows that a jet with a maximum streamwise velocity double that of the peak plunge velocity V_p is produced at $x/c = 0.41$ when the airfoil is oscillated at $U_0 = 0$ for $f = 5$ Hz and $h = 0.04$ and 0.06 . Although no systematic tests have been performed to study the role played by the sharp trailing edge, it is likely that a reasonably sharp edge is required for effective thrust generation (similar to the role played by a sharp trailing edge for lift generation on a conventional airfoil).

V. Conclusions

LDV measurements of a plunging circular cylinder at $U_0 = 0$ shows that contrary to a plunging airfoil, no jet is produced. For a plunging NACA 0012 airfoil, the mean velocity profiles, indicative of a jet, are independent of the frequency of oscillation when the jet velocity and the lateral distance are nondimensionalized by the peak plunge velocity and the amplitude of oscillation, respectively. These results are consistent with the dimensional analysis.

Acknowledgments

This work has been supported by the Office of Naval Research. The first author acknowledges partial support from the Naval Postgraduate School under the National Research Council Research Associateship Program. Assistance provided by J. Yue in acquiring some of the laser Doppler velocimetry data is acknowledged.

References

- Birnbaum, W., "Das ebene Problem des Schlagenden Flügels," *Zeitschrift fuer Angewandte Mathematik und Mechanik*, Vol. 4, No. 4, 1924, pp. 277–292.
- Theodorsen, T., "General Theory of Aerodynamic Instability and the Mechanism of Flutter," NACA TR 496, 1935.
- Garrick, I. E., "Propulsion of a Flapping and Oscillating Airfoil," NACA Rept. 567, 1936.
- Lighthill, M. J., "Note on the Swimming of Slender Fish," *Journal of Fluid Mechanics*, Vol. 9, Pt. 2, 1960, pp. 305–317.
- Koochesfahani, M. M., "Vortical Patterns in the Wake of an Oscillating Airfoil," *AIAA Journal*, Vol. 27, No. 9, 1989, pp. 1200–1205.
- Freythuth, P., "Propulsive Vortical Signatures of Plunging and Pitching Airfoils," *AIAA Journal*, Vol. 26, No. 7, 1988, pp. 881–883.
- Lai, J. C. S., and Platzer, M. F., "Jet Characteristics of a Plunging Airfoil," *AIAA Journal*, Vol. 37, No. 12, 1999, pp. 1529–1537.
- Knoller, R., "Die Gesetze des Luftwiderstandes," *Flug- und Motorteknik (Wien)*, Vol. 3, No. 21, 1909, pp. 1–7.
- Betz, A., "Ein Beitrag zur Erklarung des Segelfluges," *Zeitschrift fuer Flugtechnik und Motorluftschiffahrt*, Vol. 3, No. 21, 1912, pp. 269–272.
- Bennett, A. G., Obye, R. C., and Jeglum, P. M., "Ornithopter Aerodynamic Experiments," *Swimming and Flying in Nature*, edited by T. Y. T. Wu, C. J. Brokaw, and C. Brennen, Vol. 2, Plenum, New York, 1975, pp. 985–1000.
- Jones, K. D., Dohring, C. M., and Platzer, M. F., "Experimental and Computational Investigation of the Knoller–Betz Effect," *AIAA Journal*, Vol. 36, No. 7, 1998, pp. 1240–1246.
- Freythuth, P., "Thrust Generation by an Airfoil in Hover Modes," *Experiments in Fluids*, Vol. 9, No. 1, 1990, pp. 17–24.
- Shyy, W., Berg, M., and Ljungqvist, D., "Flapping and Flexible Wings for Biological and Micro Air Vehicles," *Progress in Aerospace Sciences*, Vol. 35, No. 5, 1999, pp. 455–506.
- Tuncer, I. H., and Platzer, M. F., "Computational Study of Flapping Airfoil Aerodynamics," *Journal of Aircraft*, Vol. 37, No. 3, 2000, pp. 514–520.